

# Polysulfone Membranes. V. Poly(phenyl sulfone) (Radel R)-Poly(vinyl pyrrolidone) Membranes\*

M. M. DAL-CIN,<sup>†</sup> C. M. TAM, M. D. GIVER, and T. A. TWEDDLE

National Research Council of Canada, Institute for Environmental Research and Technology,  
Ottawa, Ontario, Canada K1A-0R6

## SYNOPSIS

Ultrafiltration membranes were prepared from mixtures of poly(phenyl sulfone) (Radel R5000) and poly(vinyl pyrrolidone) (PVP) dissolved in 1-methyl-2-pyrrolidinone (NMP). The effects of the casting solution composition on membrane performance and morphology are presented. Radel R5000 membranes showed higher productivity for a given pore size when compared to other polysulfone membranes. The biphenyl group in Radel R5000 makes it more rigid in comparison to other polysulfones. This may result in more ordered packing, which resulted in the higher productivities and smaller pore sizes observed in the membranes. © 1994 John Wiley & Sons, Inc.

## INTRODUCTION

Synthetic membrane processes are an attractive alternative to conventional separation technologies. The basic principles of membrane separation and its commercial importance have been extensively reported.<sup>1,2</sup> Continual development of new membrane materials is crucial to sustain and expand the growing interest in this technology.<sup>3</sup>

The development of a polymer into a membrane involves a knowledge of the membrane-formation process and its relation to separation performance. The majority of synthetic membranes are made using a phase-inversion process. In this technique, the polymer is dissolved in a solvent to form a casting solution, which is spread over a porous support. The cast film of the polymer solution is immersed into a nonsolvent, causing the polymer to precipitate and an asymmetric membrane to form. The composition of the casting solution and the method of gelation contributes to the membrane's properties.<sup>4</sup> Performance comparisons between different membranes are based on pore size and productivity. Optimization of this performance is based on the ability to control the structure of the membrane surface.

Radel R5000, one of several commercially available polysulfones, is an ideal candidate for consideration as a membrane material. Polysulfones are

high-performance polymers suitable for operation in harsh environments and high temperatures.<sup>5</sup> A large proportion of commercial ultrafiltration membranes are made from bisphenol A polysulfones (Udel) or polyethersulfones (Victrex PES) because of their desirable film-forming, physical, and chemical attributes. The solution and viscoelastic melt properties of Radel R5000 were reported by Roovers et al.<sup>6,7</sup> However, there have been virtually no published reports on its ultrafiltration membrane properties, even though this polymer has favorable attributes similar to other polysulfones. Recently, Aitken et al.<sup>8</sup> reported on the gas transport properties of poly(phenyl sulfone).

In this study, poly(phenyl sulfone) (Radel R5000) was evaluated as a material for ultrafiltration membranes. Casting solutions were made from Radel R and poly(vinyl pyrrolidone) (PVP) polymers and dissolved in *N*-methyl-2-pyrrolidinone (NMP). PVP was used as an additive to control the casting solution viscosity and membrane properties. The variation of casting solution viscosity, membrane pore size, and membrane porosity are described as a function of the casting solution composition.

## EXPERIMENTAL

### Materials

Poly(phenyl sulfone) (Radel-R5000) was obtained from Amoco Performance Products, Inc. Radel R was dried at 120°C overnight before use. Reagent-

\* Issued as NRC No. 35781.

† To whom correspondence should be addressed.

grade *N*-methyl-2-pyrrolidinone (NMP) was obtained from Anachemica and used as received. Poly(vinyl pyrrolidone) (PVP 10,000 MW) was obtained from Sigma and was dried overnight at 25°C in a vacuum oven. Different molecular weight polyethylene glycols (PEG) ranging from 600 to 35,000 daltons were obtained from Fluka and used as solutes in the sieving experiments. The chemical structures of poly(phenyl sulfone) and several other polysulfones are given in Figure 1.

### Membrane Preparation

Three-component membrane casting solutions were made from Radel R and PVP dissolved in NMP solvent. Casting solution compositions were from all combinations of Radel R at 15, 20, and 25 wt % and PVP at 0, 5, 10, 15, 20, and 25 wt %. A Haaka (M500) viscometer was used to measure the zero shear viscosities at 25°C.

Membranes were fabricated on a mechanical casting machine by casting a film of a polymer solution 254 µm (0.010 in) thick onto a spun-bound polyester backing (Hollitex 3296). Membranes were gelled in reverse osmosis purified water at 4°C and were kept in water that was replaced each day for a 5 day period to remove residual NMP. A 25 vol % ethanol-75 vol % water mixture was used for long-term storage until used.

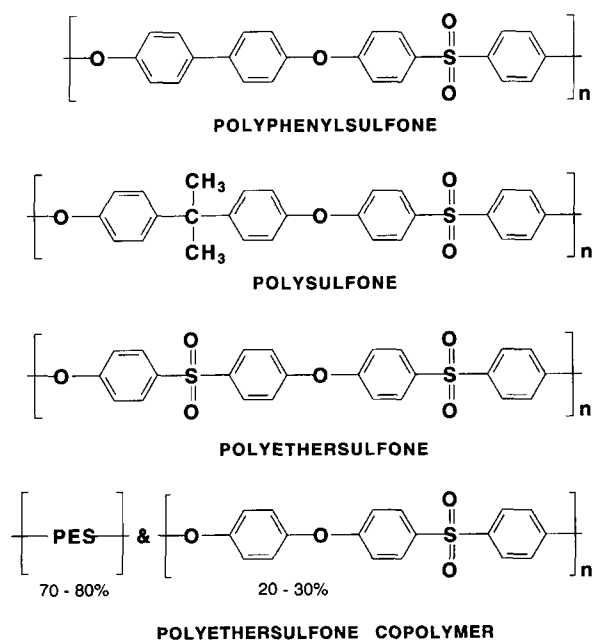


**Figure 1** Structural repeating unit of Radel R5000 poly(phenyl sulfone) and other polysulfones.

### Membrane Characterization

Ultrafiltration experiments were performed in thin-channel cross-flow test cells with an effective membrane surface area of  $14.5 \times 10^{-4} \text{ m}^2$ . A cross-flow velocity of 0.8 m/s over the membrane surface ensured operation in turbulent flow. Separation experiments were carried out at an operating pressure of 344 kPa (50 psig) or 69 kPa (10 psig) depending on the average pore radius of the membrane.

Membranes were prepressurized at the operating pressure for 5 h to ensure complete removal of any mobile PVP, NMP, or ethanol and to compact the membrane. A PEG feed concentration of 200 mg/L was used for the solute sieving experiments. The combination of low feed concentration and turbulent flow conditions reduced the possibility of concentration polarization at the membrane surface. Feed and permeate concentrations of PEG were determined using an automated Shimadzu 5000 Total Organic Carbon analyzer.

Scanning electron microscopy (SEM) cross sections of some of the membranes were obtained with a JEOL microscope. Dried membranes were fractured in liquid nitrogen and coated with gold under vacuum.

## RESULTS AND DISCUSSION

### Casting Solution Viscosity

Polymer solution viscosity is an important consideration for casting flat-sheet membranes. To some extent, this controls the penetration of the casting solution into the backing material. Other factors controlling penetration include the casting speed, film thickness, and standing time. Fabricating hollow fiber membranes requires considerably higher viscosities, since the nascent pregelled fiber is supported only by the viscosity of the extruded solution.<sup>9</sup>

The viscosity data for different concentrations of Radel R and PVP are represented by a three-dimensional surface plot [Fig. 2(a)] and an associated contour plot [Fig. 2(b)]. The logarithm of the viscosity was used to accommodate the large range of data. In this and other similar figures, the experimental results are represented by solid circles. The surface itself is the predicted value obtained from a linear least-squares-fitted polynomial. The vectors locate a given data point on the surface. The maximum viscosity for a Radel R/NMP polymer solution was 17.3 Pa·s for a 25.0 wt % solution. The Radel R solution viscosity was increased by the addition of PVP. Viscosities of up to 2000 Pa·s were

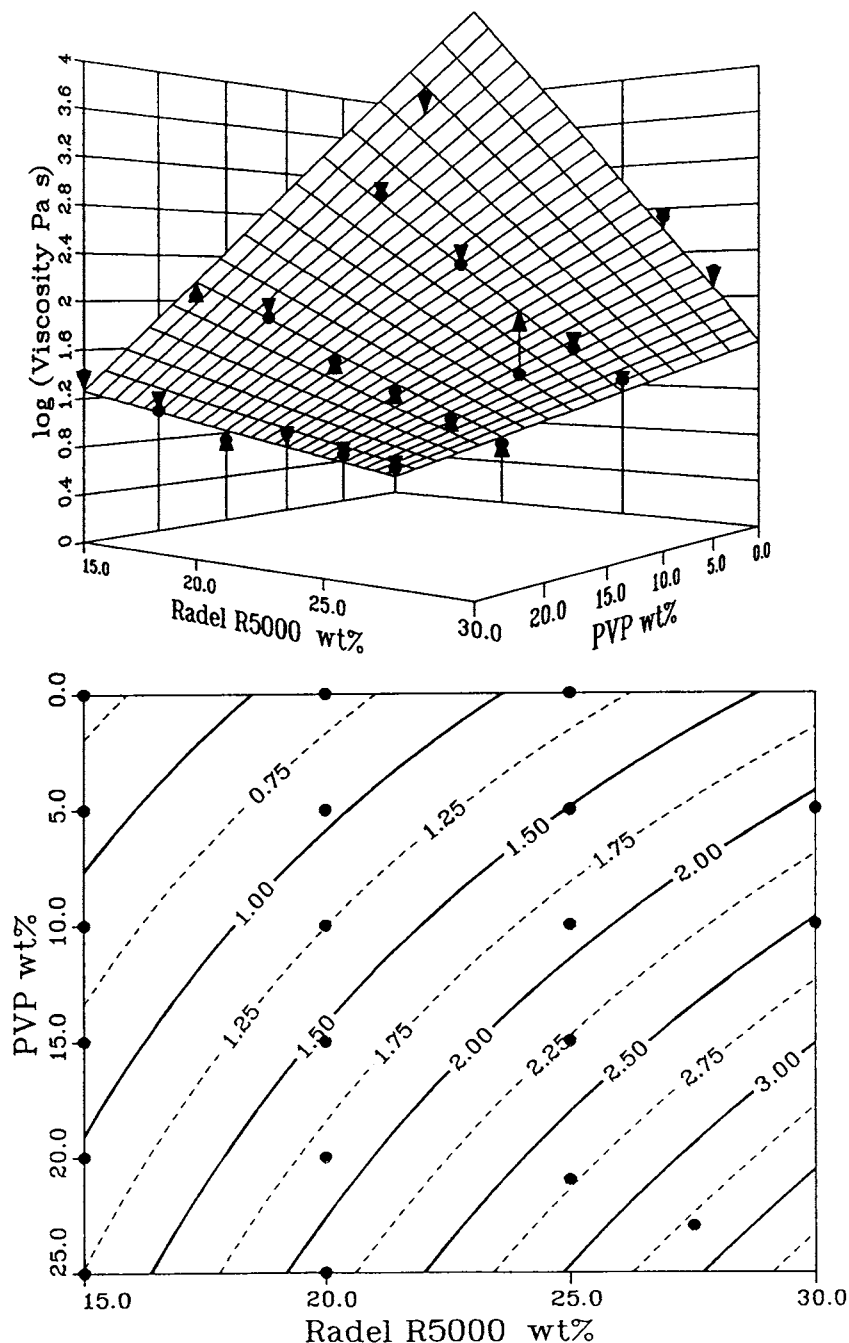


**Figure 2** (a) Logarithmic surface plot of Radel R5000/PVP casting solution viscosity as a function of composition. Surface obtained from a polynomial fitted to experimental data (●) using sum of squares of residuals. (b) Figure 2(a) presented as a contour plot.

obtained for a 27.5/23 wt % Radel R/PVP casting solution.

Radel R casting solutions had higher viscosities than did those observed with other polysulfones. A 15 wt % Radel R solution in NMP had a viscosity of 1.76 Pa·s. In comparison, the viscosity of a Radel A100 solution was only 0.22 Pa·s (Ref. 10) for the

same concentration. This enables membranes to be cast using lower concentrations of Radel R.

#### Membrane Morphology: Pore Size

The membrane morphology was influenced by both the casting solution composition and viscosity. Fig-

ure 3 is a series of SEMs of Radel R/PVP membranes made from casting solutions of moderate viscosity. The micrographs show typical "fingerlike" voids beneath the skin layer. The shape and structure were related to the concentration of polymer and additive in the casting solution. When the polymer concentration was low, less than  $\sim 15\%$  [Fig. 3(a)], the fingerlike voids were not well defined. When the polymer concentration (and, consequently, the viscosity) was increased, the number of voids decreased while their size and the thickness of the walls between voids increased [Fig. 3(a)-(c)]. A comparison of Figure 3(a) with Figure 3(d) and Figure 3(b) with Figure 3(e) shows that this type of morphology was also achieved when the PVP content was increased. At higher solution viscosities, the fingerlike voids were absent and replaced by a thick sponge layer (Fig. 4).

The creation of macroscopic structures is related to the rate of membrane formation. A fast exchange between the solvent-polymer phase and the water tends to result in fingerlike voids. Conversely, a slow exchange rate results in spongelike structures.<sup>11,12</sup>

In Figure 3(a)–(d) and Figure 3(b)–(e), a more distinct void structure was obtained with higher solution viscosities. However, in these cases, the solvent–nonsolvent exchange was facilitated by the presence of water-soluble PVP. At higher polymer concentrations, the effect of PVP was less pronounced. The effect of faster water–NMP exchange was offset by the higher solution viscosity, which tended to promote a slow solvent–nonsolvent exchange.

The membrane pore size ( $r_p$ ) can be obtained from PEG separation ( $f$ ) by<sup>13</sup>

$$f = 1 - \frac{\chi}{1 - e^{-Pe}(1 - \chi)} \quad (1)$$

The pore Peclet number,  $Pe$ , is the ratio of the convective and diffusive transport of the solute through the pore. Both types of solute flow account for the influence of the pore wall as the solute size approaches the pore size. A global steric parameter ( $\chi$ ) associated with the restricted convective trans-

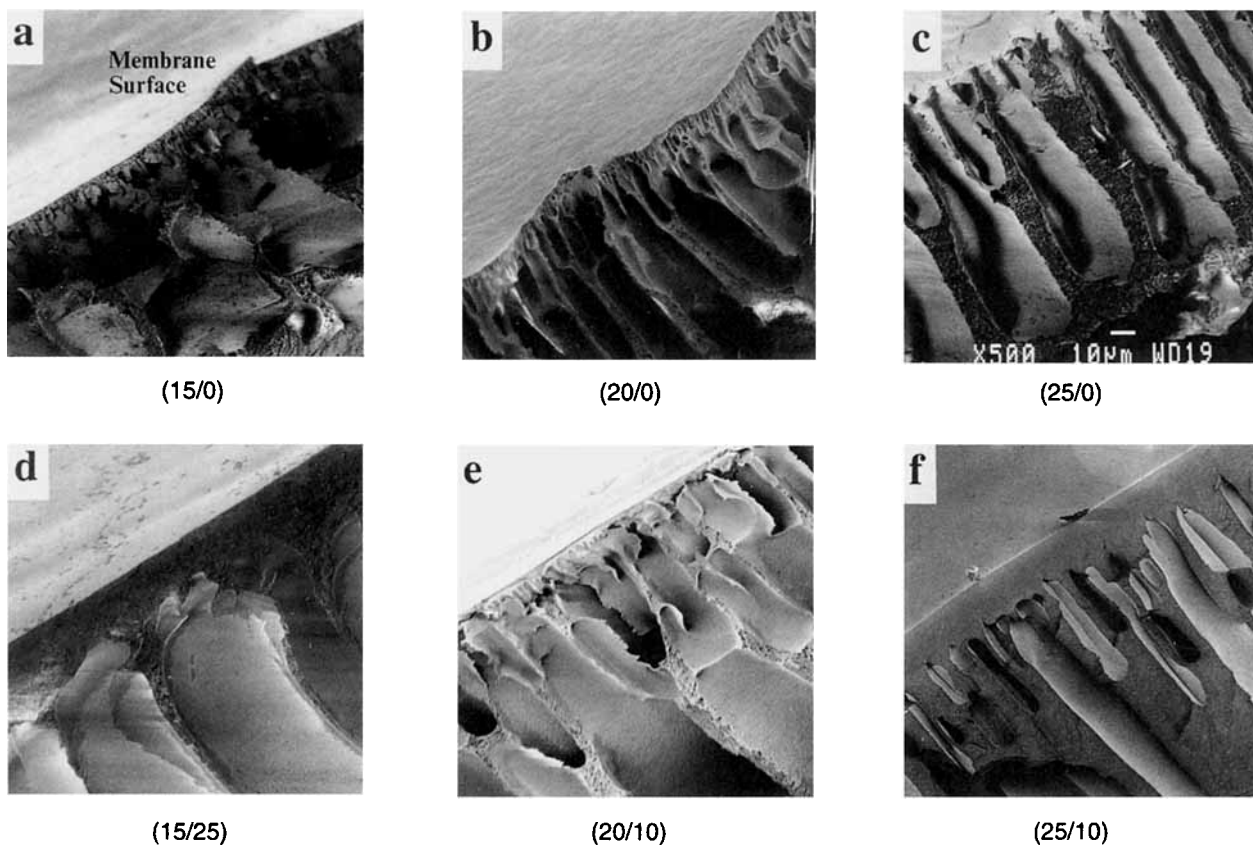


**Figure 3** SEM micrographs of Radel R/PVP membranes for given casting solution compositions (wt % Radel R/wt % PVP).

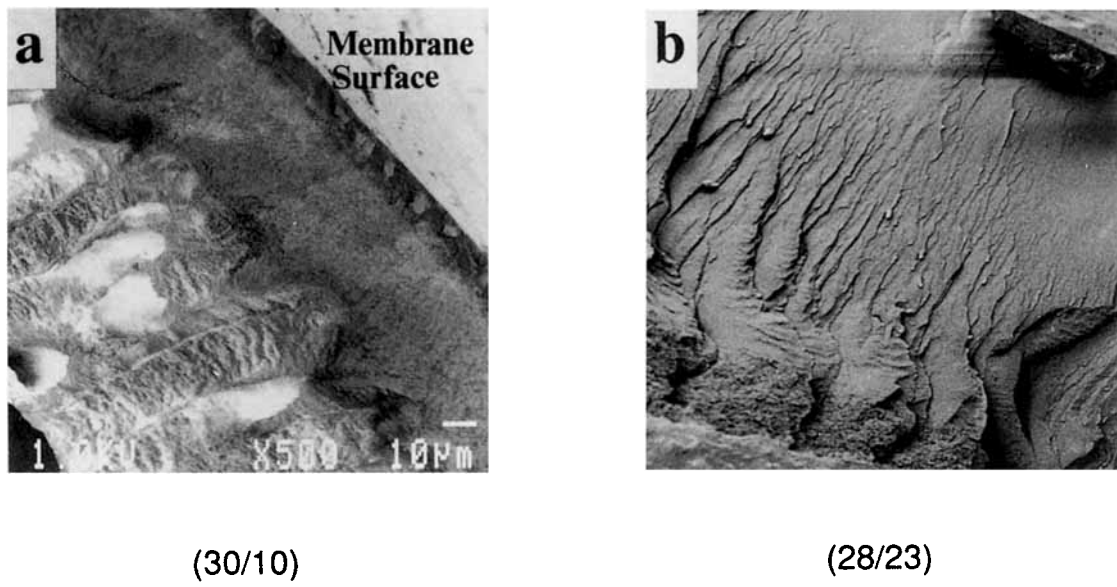


**Figure 4** SEM micrographs of Radel R/PVP membranes for high-viscosity casting solutions (wt % Radel R/wt % PVP).

port within the pore and a ratio of restricted diffusivity ( $\xi$ ) of the solute within the pore to the bulk diffusivity of the solute are calculated numerically.<sup>14</sup> The Peclet number can be defined as

$$Pe = \frac{\chi}{\xi D_\alpha} \left[ \frac{r_p^2 \Delta P}{8\eta} \right] \quad (2)$$

The viscosity of water is  $\eta$  and  $\Delta P$  is the pressure drop across the membrane. Typical experimental

separation data and predicted separations for several membranes are shown in Figure 5.

The average pore size of a membrane is related to the casting solution composition as shown in Figure 6(a) and (b). The contour plots show that the average pore size is related to the concentration of both Radel R and PVP. An increase in the concentration of either one or both components results in a decrease in pore size. This casting solution system was capable of producing membranes with an av-

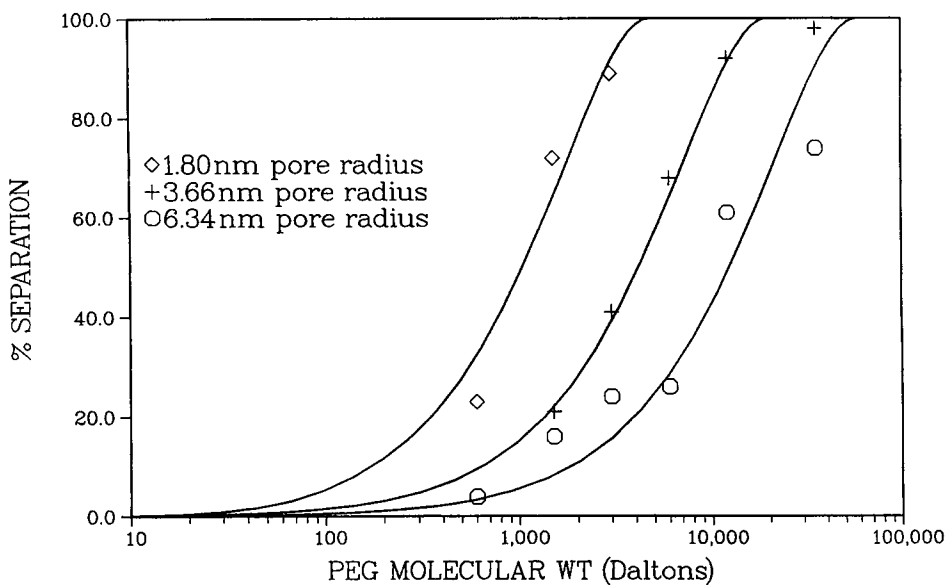


**Figure 5** Typical experimental and predicted separation data for three Radel R wt % / PVP wt % membranes: ( $\diamond$ ) 25/15; (+) 20/15; (O) 20/5.

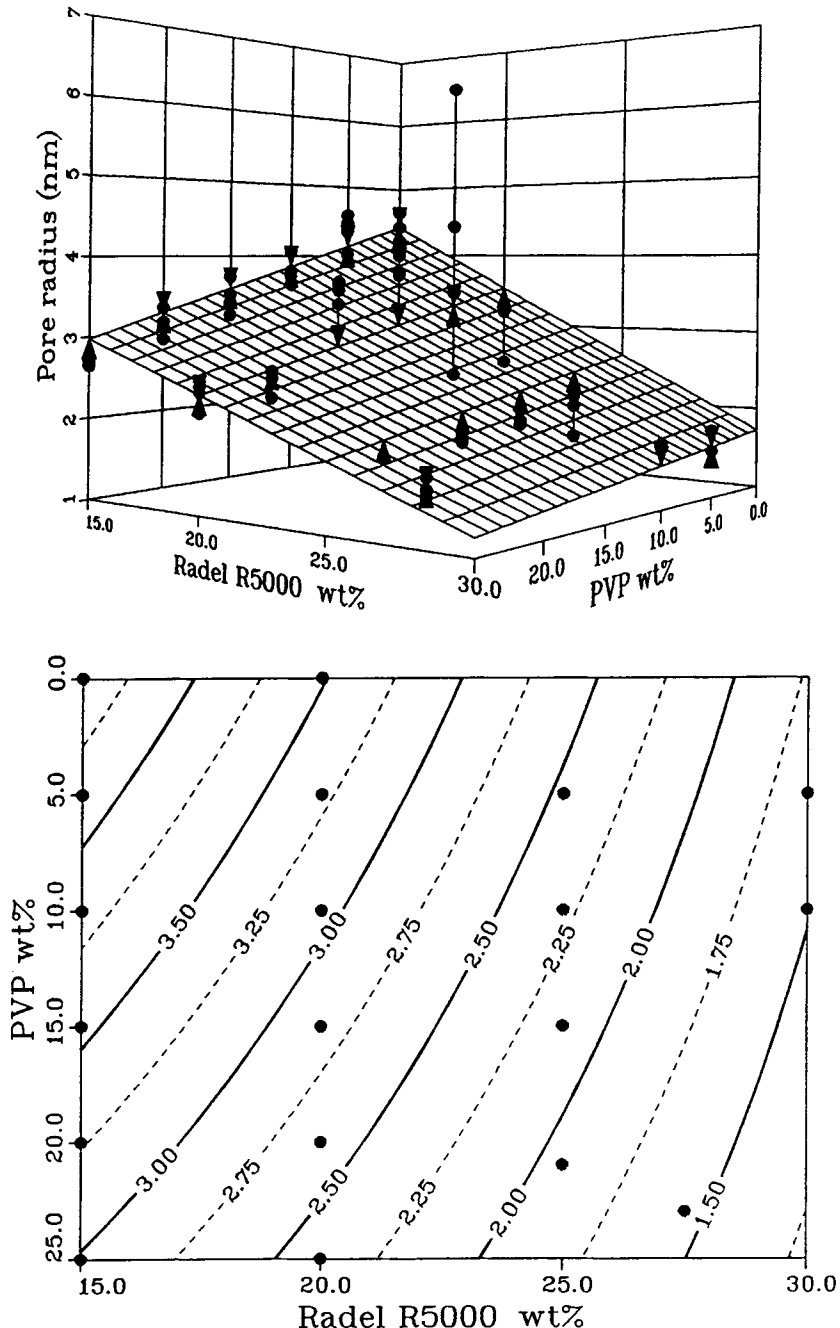


**Figure 6** (a) Surface plot of pore size as a function of casting solution composition. Surface obtained from a polynomial fitted to experimental data (●) using sum of squares of residuals. (b) Figure 6(a) presented as a contour plot.

verage pore radius of less than 1.5 nm. The effect of PVP was more pronounced at the lower Radel R concentrations. These trends have been observed in previous studies.<sup>10,15</sup>

The pore-size range of Radel R membranes was considerably narrower for similar compositions than for other polysulfones. Radel R pore sizes ranged

from 1.5 to 4.0 nm, whereas the ranges for Udel P3500, Victrex 200P, and Radel A100 were 2.0–13 nm, 2.7–12 nm, and 2.5–78 nm, respectively. Radel R membranes also had the smallest absolute pore size. Due to the higher viscosity of Radel R casting solutions, more open membranes may have been made with casting solutions having a lower Radel

R and/or PVP concentration. However, this is not part of the present work.

### Membrane Morphology: Permeability

A parameter characterizing the combined effects of a membrane's porosity and resistance to flow can be obtained from the pure water permeation (PWP) rate once the pore radius ( $r_p$ ) has been determined from solute sieving experiments.<sup>16</sup> Rearranging the Hagen-Poiseuille equation, a ratio of the number of pores ( $n$ ) to the pore length ( $\Delta x$ ) per unit area ( $A$ ) that is proportional to the volumetric flow rate ( $Q$ ) can be obtained so that

$$\frac{n}{\Delta x A} = \frac{8Q\eta}{\pi \Delta P r_p^4 A} \quad (3)$$

This is a convenient measure of a membrane's performance for a given pore size. High fluxes can be the result of both large pores and high porosity. These two effects cannot be distinguished by measuring only the PWP. The relationship between the casting solution composition and membrane performance cannot be based on the PWP alone. However, a physical explanation involving the changing characteristics of the membrane's performance and structure can be applied if we assume the validity of the Hagen-Poiseuille law and determine a per-

meability value. The physical significance of this parameter remains valid even though it is extremely sensitive to estimates of the pore radius as well as to variations in PWP.

The formulations of 15/25 wt % and 20/10 wt % solutions had similar PWP's but different pore radii at 2.69 and 4.20 nm, respectively (Table I). The differences in membrane morphology for these two casting solutions is reflected in the ratio  $n/\Delta x A$ :  $184.0 \times 10^{21} \text{ m}^{-3}$  and  $30.3 \times 10^{21} \text{ m}^{-3}$ , respectively. This indicates either a higher number of pores or a lower effective pore length for the 15–25 solution.

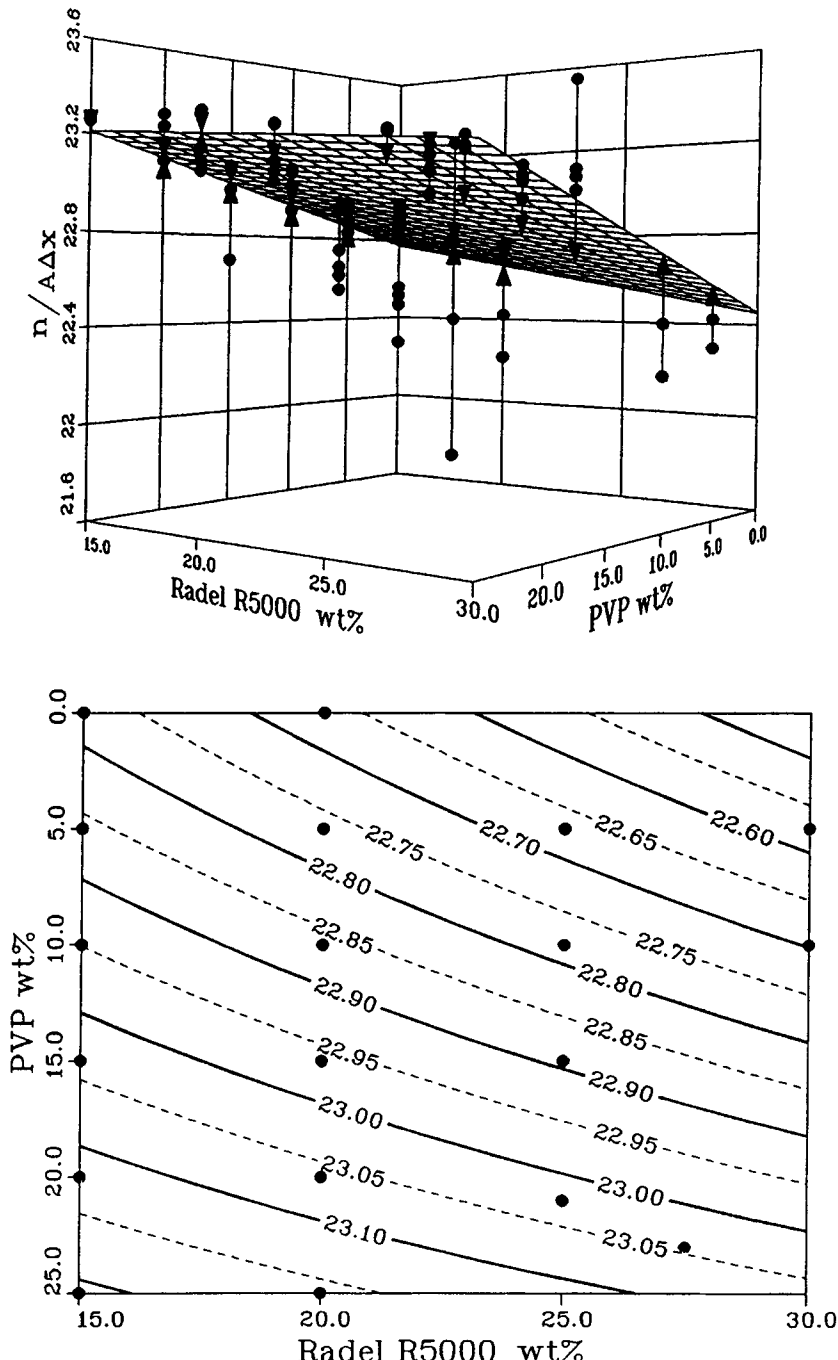
Increasing the PVP concentration at 15 wt % Radel R decreased both the PWP's and pore radius. The PWP's is the combination of two parameters: the pore radius and  $n/\Delta x A$ . The decreasing PWP's could have been the result of either smaller pore sizes or lower porosity. However, evaluation of the ratio  $n/\Delta x A$  clearly indicates that the reduced pore size is partially compensated by an increasing pore density ( $n/A$ ) or, less likely, by a shorter effective pore length ( $\Delta x$ ). This trend was also observed at a Radel R concentrations of 20%. There was little change in PWP's,  $n/\Delta x A$ , or the pore radius at a Radel R concentration of 25 wt %.

Figure 7(a) and (b) show the effect of the casting solution composition on the ratio  $n/\Delta x A$ . The contour plots show the importance of adding PVP to the casting solution. High  $n/\Delta x A$  ratios could only be achieved with high concentrations of PVP. For

**Table I Casting Formulations of Radel R 5000 and Their Respective Performance Parameters**

Formulation (Wt % Radel R-Wt % PVP)	Pore Radius (nm)	$n/\Delta x A$ ( $\text{m}^{-3} \times 10^{-21}$ )	TMP (psig)	PWP <sub>s</sub> $\text{L}/(\text{m}^2 \text{ h atm})$
15-0	$4.00 \pm 0.80$	$82.2 \pm 31.5$	10	$474.7 \pm 234.2$
15-5	$4.35 \pm 0.59$	$74.7 \pm 32.9$	10	$612.8 \pm 74.1$
15-10	$3.78 \pm 0.47$	$113.0 \pm 50.1$	10	$530.2 \pm 50.9$
15-15	$3.43 \pm 0.52$	$101.0 \pm 86.4$	10	$324.0 \pm 280.8$
15-20	$3.12 \pm 0.50$	$168.0 \pm 97.2$	10	$364.1 \pm 35.1$
15-25	$2.69 \pm 0.09$	$184.0 \pm 10.6$	10	$225.2 \pm 19.8$
20-0	$2.95 \pm 1.04$	$33.7 \pm 51.5$	50	$51.2 \pm 41.5$
20-5	$4.13 \pm 4.00$	$65.3 \pm 172.2$	50	$191.2 \pm 119.7$
20-10	$4.20 \pm 0.59$	$30.3 \pm 16.2$	50	$213.4 \pm 10.0$
20-15	$3.55 \pm 0.31$	$43.7 \pm 17.0$	50	$161.8 \pm 49.5$
20-20	$2.49 \pm 0.35$	$141.0 \pm 76.2$	50	$124.7 \pm 49.4$
20-25	$2.41 \pm 0.38$	$131.0 \pm 78.8$	50	$99.7 \pm 8.1$
25-5	$1.99 \pm 0.61$	$159.0 \pm 228.9$	50	$51.1 \pm 17.6$
25-10	$1.93 \pm 0.19$	$104.0 \pm 32.5$	50	$33.2 \pm 4.2$
25-15	$1.80 \pm 0.07$	$138.0 \pm 19.5$	50	$33.7 \pm 7.2$
25-21*	$1.74 \pm 0.06$	$144.0 \pm 27.8$	50	$32.8 \pm 19.6$

Pore sizes,  $n/\Delta x A$ , and PWP's represent the average of four coupons (\* represents the average of two) and 90% confidence intervals.



**Figure 7** (a) Logarithmic plot of  $n/\Delta xA$  as function of casting solution composition. Surface obtained from a polynomial fitted to experimental data (●) using sum of squares of residuals. (b) Figure 7(a) presented as a contour plot.

example,  $n/\Delta xA$  increased from  $5.85 \times 10^{22} \text{ m}^{-3}$  to  $10.8 \times 10^{22} \text{ m}^{-3}$  by adding 20% PVP to a 20% Radel R solution. PVP has been found to have similar effects on membranes produced from other polysulfones.<sup>15,17,18</sup> PVP is water-soluble and, for the most part, is removed from the membrane by the gelation

media. This produces more pores in the membrane and, consequently, increases the  $n/\Delta xA$  ratio.

The concentration of Radel R had little effect on  $n/\Delta xA$  when compared to the effect of PVP. For example, without PVP,  $n/\Delta xA$  for a membrane prepared from a 15% polymer solution was 6.03

$\times 10^{22} \text{ m}^{-3}$ . By comparison, a 30% solution produced membranes with  $n/\Delta x A = 2.82 \times 10^{22} \text{ m}^{-3}$ . The decrease in  $n/\Delta x A$  for increasing Radel R concentrations was unexpected. In general, for membranes made from other polysulfones,  $n/\Delta x A$  increased with increasing polymer chain density (polymer concentration). The variation of  $n/\Delta x A$  with Radel R concentration was small enough that it can be considered constant, particularly considering the variation seen with other polysulfones.<sup>10,15</sup> In these cases,  $n/\Delta x A$  typically varied by two orders of magnitude.

The weak correlation between  $n/\Delta x A$  and the Radel R concentration may be due to its relatively high polymer chain rigidity. This lack of flexibility is due to the presence of the biphenyl group that hinders movement of the polymer chain (Fig. 1). In good solvents and at high concentrations, the polymer chains can be packed in a more regular manner. This was suggested by the higher viscosities observed for given concentrations of Radel R. Regular packing results in both smaller pores and a larger number of pores ( $n$  is large). This higher chain packing occurred at lower Radel R concentrations compared to other polysulfones. When the concentration of Radel R was increased, relatively little increase in the packing density was observed. The lowest  $n/\Delta x A$  observed with any Radel R casting solution ( $9.6 \times 10^{22} \text{ m}^{-3}$ ) surpassed the highest  $n/\Delta x A$  obtained with Radel A ( $4.8 \times 10^{22} \text{ m}^{-3}$ ) and Victrex

200P ( $4.6 \times 10^{22} \text{ m}^{-3}$ ) and approached that of Udel P3500 ( $1.2 \times 10^{23} \text{ m}^{-3}$ ).

As the Radel R concentration was increased, the morphology of the gelled membrane also changed. In particular, the effective pore length,  $\Delta x$ , increased at a faster rate than did  $n$ . This was supported by the SEM micrographs. Although the actual pores cannot be identified, the layer immediately below the membrane changed from an open sponge structure to a very dense layer that became indistinguishable from the skin. The net effect was the reduction of  $n/\Delta x A$ .

### Radel R5000: Performance Comparisons

A method for comparing membrane performance is to plot  $n/\Delta x A$  as a function of the pore radius. This allows one to determine which membranes would have the highest flux for a given pore size. Figure 8 compares Radel R membrane performance with that of other polysulfones discussed in this work and several commercial membranes. As discussed earlier, the limited range of pore sizes obtained with Radel R for a wide range of casting solution formulations is clearly evident. Also, of greater importance is that Radel R membranes have higher porosities for the pore radius range of 1.5 to  $\sim 4.0$  nm. By recalling that the porosity is plotted on a logarithmic axis, these productivities are significantly higher.

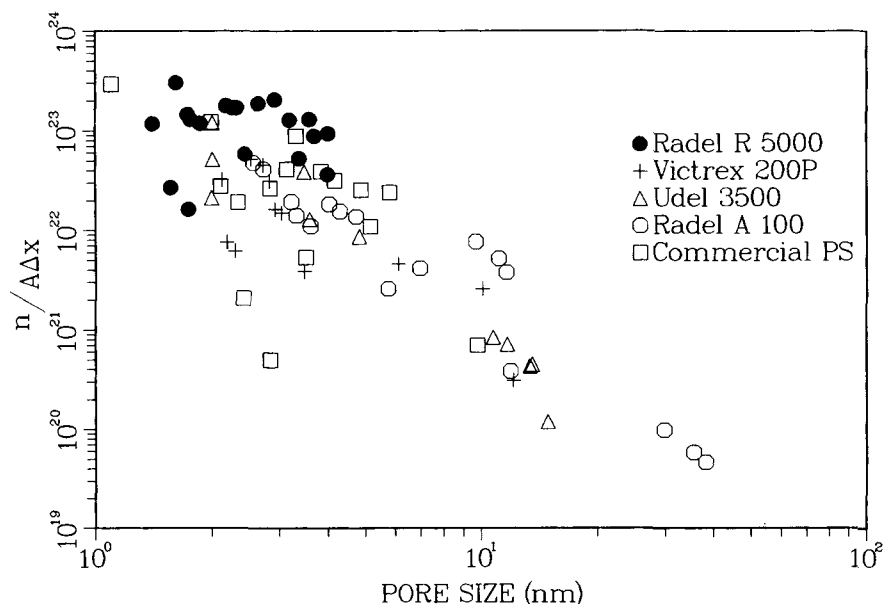


**Figure 8** A plot of  $n/\Delta x A$  as a function of the pore radius for Radel R/PVP and other commercial and NRC polysulfone membranes.

## CONCLUSIONS

A systematic exploration of casting solution formulations using Radel R/PVP/NMP was used to produce ultrafiltration membranes. This system produced membranes with similar structural features as those of other polysulfone membranes, as shown by SEM micrographs. However, the performance characteristics of Radel R membranes differed from those of the other polysulfone membranes.

A systematic exploration of casting solution formulations is desirable in order to control membrane performance. This approach identifies the roles of Radel R and PVP in determining membrane performance. Increasing the Radel R concentration resulted in lower  $n/\Delta x A$  ratios and smaller pore sizes. Increasing the PVP content also reduced the pore size but increased the  $n/\Delta x A$  ratio.

Ultrafiltration membranes made with Radel R had higher  $n/\Delta x A$  ratios for a given pore size. In practice, this would result in membranes with higher fluxes or allow operation at lower pressures without sacrificing productivity. These features could result in considerable cost savings in large-scale applications. The pore-size range obtained with Radel R membranes was smaller than with other polysulfones. In addition, smaller absolute pore sizes, down to a minimum of 1.5 nm, were obtained.

These differences may be attributed to the presence of the biphenyl group in Radel R. The biphenyl group, which is absent in other polysulfones, increases the polymer's chain rigidity, resulting in more ordered packing. This would account for the smaller pore sizes obtained and the narrower range of pore sizes.

The authors would like to thank G. Pleizier for the SEM micrographs of the membranes.

## NOMENCLATURE

$A$	effective permeation area of membrane ( $\text{m}^2$ )
$D_\infty$	diffusivity of solute in solution ( $\text{m}^2/\text{s}$ )
$f$	separation
$n$	number of pores
$Pe$	Peclet number
PWP	pure water permeation rate ( $\text{L}/(\text{m}^2 \text{ h})$ )
PWP <sub>s</sub>	pressure independent pure water permeation rate ( $\text{L}/(\text{m}^2 \text{ h atm})$ )
$Q$	volumetric flow rate ( $\text{m}^3/\text{h}$ )
$r_p$	pore radius (nm)
TMP	transmembrane pressure (psi or atm)

## Greek

$\Delta x$	effective length of the membrane pore (m)
$\xi$	ratio of restricted diffusion within the pore to free diffusion in bulk solution
$\eta$	viscosity (Pa-s)
$\chi$	global steric parameter
$\Delta P$	pressure drop across the pore (kPa)

## REFERENCES

1. H. K. Lonsdale, *J. Membr. Sci.*, **10**, 81–181 (1982).
2. A. Crull, *Membranes for the Nineties: Highlighting Surface Modification Technology*, Business Communications Co., Norwalk, CT, 1990.
3. *Membrane Separation Systems—A Research and Development Needs Assessment*, DOE/ER/30133, March 1990.
4. S. Sourirajan and T. Matsuura, *Reverse Osmosis and Ultrafiltration Process Principles*, National Research Council of Canada, Ottawa, 1989.
5. J. E. Harris and R. N. Johnson, in *Encyclopedia of Polymer Science and Engineering*, Wiley, New York, **13**, 196–211 (1989).
6. J. Roovers, R. Ethier, and P. M. Toporowski, *High Performance Polym.*, **2**(3), 151–163 (1990).
7. J. Roovers, P. M. Toporowski, and R. Ethier, *High Performance Polym.*, **2**(3), 165–179 (1990).
8. C. L. Aitken, W. Koros, and D. Paul, *Macromolecules*, **25**, 3641–3658 (1992).
9. I. Cabasso, E. Klein, and J. E. Smith, *J. Appl. Polym. Sci.*, **20**, 2377–2394 (1976).
10. C. M. Tam, M. Dal-Cin, and M. D. Guiver, *J. Membr. Sci.*, **78**, 123–134 (1993).
11. H. Strathmann, in *Synthetic Membranes: Science, Engineering and Applications*, P. M. Bungay, H. K. Lonsdale, and M. N. de Pinho, Eds., NATO ASI Series 181, D. Reidel, Dordrecht, 1986.
12. S. Munari, A. Buttino, G. Capannelli, P. Moretti, and P. Petit Bon, *Desalination*, **70**, 265–275 (1988).
13. C. M. Tam and A. Y. Tremblay, *J. Membr. Sci.*, **57**, 271–287 (1991).
14. J. Happel and H. Brenner, *Low Reynolds Number Hydrodynamics*, Martinus Nijhoff, Dordrecht, 1986.
15. C. M. Tam, A. Tweddle, O. Kutowy, and J. D. Hazlett, *Desalination*, **89**, 275–287 (1993).
16. A. Tweddle, C. Striez, C. Tam, and J. D. Hazlett, *Desalination*, **86**, 27–41 (1991).
17. L. Lafrenière, F. D. F. Talbot, T. Matsuura, and S. Sourirajan, *Ind. Eng. Chem. Res.*, **26**, 2385–2389 (1987).
18. T. Miyano, T. Matsuura, and S. Sourirajan, *Chem. Eng. Commun.*, **119**, 23–39 (1993).

Received January 26, 1994

Accepted February 27, 1994